

Bimetallic Complexes of Ytterbium and Europium Stabilized by Sterically Demanding Dipyriddydamides

Anna M. Dietel,^[a] Christian Döring,^[a] Germund Glatz,^[a] Mikhail V. Butovskii,^[a]
Oleg Tok,^[a] Falko M. Schappacher,^[b] Rainer Pöttgen,^[b] and Rhett Kempe*^[a]

Keywords: Lanthanides / Europium / Ytterbium / Moessbauer spectroscopy / N ligands / ¹⁷¹Yb NMR spectroscopy

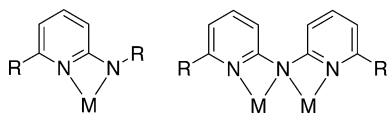
Deprotonation of Ap*pyH {Ap*pyH = (6-methylpyridin-2-yl)-[6-(2,4,6-triisopropylphenyl)-pyridin-2-yl]-amine} using KH leads to Ap*pyK which undergoes a clean salt metathesis reaction with [YbI₂(thf)₄] and [EuI₂(thf)₄] in THF forming [Yb₂(Ap*py)₃I(thf)] and [Eu₂(Ap*py)₃I(thf)], respectively. The two Yb^{II} centers in [Yb₂(Ap*py)₃I(thf)] are in close proximity and chemically different. Thus, an f-block-element–f-block-element coupling pattern was observed. The low-field ¹⁷¹Yb signal consists of a central singlet and two satellites with integral intensities of about 7 % each. This 14 % approximately corresponds to the natural abundance of the ¹⁷¹Yb isotope and was assigned as a doublet arising from ¹J(¹⁷¹Yb, ¹⁷¹Yb) spin-spin coupling with a magnitude of 76.1 Hz. The ¹⁵¹Eu Mössbauer spectrum of [Eu₂(Ap*py)₃I(thf)] recorded at 77 K shows an isomer shift (δ) of –11.9(1) mm/s with an experimen-

tal line width (I) of 6.9(1) mm/s. This line width is extremely large and results from an overlap of the signals from both crystallographically independent europium sites. The reaction of [Yb₂(Ap*py)₃I(thf)] with Ap*pyK leads to [Yb₂(Ap*py)₄(thf)₂]. In the reactions of [Yb₂(Ap*py)₃I(thf)] with azidotrimethylsilane and sulfur the rearrangement products [Yb₂(Ap*py)₃I₂] and [Yb₂(Ap*py)₃I₃] were obtained, respectively. Treating [Yb₂(Ap*py)₃I(thf)] with NaN(SiMe₃)₂ afforded homoleptic “ate” complex Na₂[Yb(Ap*py)₄]. A mixed silylamide dipyriddydamide complex was obtained in the reaction of NaYb[N(SiMe₃)₂]₃ with Ap*pyH. All complexes – three of which are paramagnetic – were characterized by X-ray crystal structure analysis.

(© Wiley-VCH Verlag GmbH & Co. KGaA, 69451 Weinheim, Germany, 2009)

Introduction

We have been continuously exploring the coordination chemistry of aminopyridinato ligands (Ap, Scheme 1, left)^[1] and started recently an extensive research program in which very bulky Ap ligands were studied.^[2] Owing to steric demand in these ligands the stabilization of mono(aminopyridinato) complexes of rare-earth elements became possible and it has been shown that small steric variations of the Ap ligands may have large synthetic, structural, and catalytic consequences.^[2]



Scheme 1. Aminopyridinato and dipyriddydamido ligands [R = (bulky) substituents].

In order to extend these investigations towards homobimetallic compounds we became interested in bulky dipyr-

iddydamides (Scheme 1, right). The parent dipyriddydamido ligand has been used successfully by Müller-Buschbaum and co-workers in the synthesis of homoleptic rare-earth dipyriddydamides.^[3] High-temperature melt synthesis has proven to be a suitable way to obtain homoleptic complexes. Because of the solvent-free character of these reactions the coordination of solvent molecules can be avoided. Deacon, Junk and co-workers reported that recrystallization of the homoleptic eight-coordinate dimeric hexa(dipyriddydamido) complex of La in THF/toluene afforded solvent-free homoleptic 10-coordinate isomer.^[4] The absence of THF in the 10-coordinate isomer was attributed to the strength of the coordination of the pyridine moiety of the dipyriddydamido ligands. These reports indicate that the solution chemistry of the parent dipyriddydamide remains rather unexplored and research into the coordination chemistry of sterically finetuned dipyriddydamides has only just begun.^[5]

Solution-state NMR has been applied infrequently to the direct observation of compounds of f-block elements owing to the fact that the majority of the complexes (except those of La^{III}, Yb^{II}, and Lu^{III}) are paramagnetic, and many of the NMR-active f-block nuclei have large quadrupole moments. An f-block-element–f-block-element coupling pattern, if observed, could be a highly sensitive probe into the dynamic aspect of f-block-element–f-block-element interactions in solution, an area of chemistry difficult to ac-

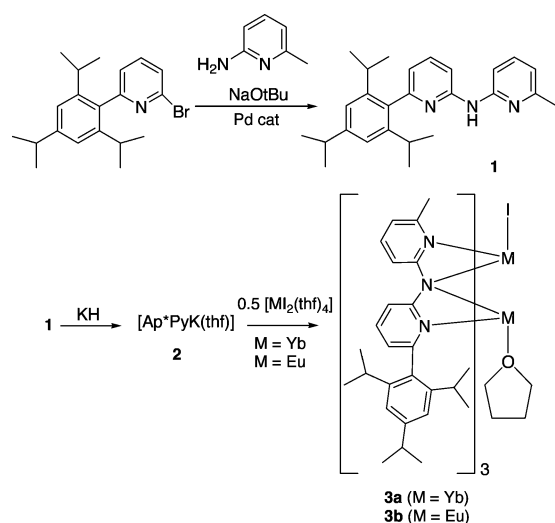
[a] Lehrstuhl Anorganische Chemie II, Universität Bayreuth, 95440 Bayreuth, Germany
Fax: +49-921-55-2157
E-mail: Kempe@Uni-Bayreuth.de

[b] Institut für Anorganische und Analytische Chemie, Westfälische Wilhelms-Universität Münster, Corrensstraße 30, 48149 Münster, Germany

cess by other methods. To observe such coupling patterns an f-block element dinuclear complex must meet two requirements: the metals must be close enough and must be in different chemical environments. Dinuclear and polynuclear Yb complexes are well-documented and the metal centers in many of them are close enough (3.5 Å was used as the upper limit)^[6] to observe ^{171}Yb – ^{171}Yb coupling. Unfortunately, these complexes are mainly highly symmetric or might become highly symmetric in solution through fast (neutral) ligand exchange. Herein we report on the synthesis, structure, and reaction chemistry of novel dinuclear Yb^{II}, Yb^{III}, and Eu^{II} complexes with sterically demanding dipyrindylamido ligands. In one of the Yb^{II} complexes the metal centers are in close proximity and chemically different within the NMR time scale – a prerequisite condition to observe $^1J(^{171}\text{Yb}, ^{171}\text{Yb})$. An Eu^{II} analog of this complex is expected to show two isomer shifts for chemically different europium sites in ^{151}Eu Mössbauer spectroscopy. The ^{171}Yb NMR spectroscopy of the Yb^{II} complex and ^{151}Eu Mössbauer spectroscopy of the Eu^{II} complex are presented. A preliminary report on such Yb^{II} compounds has been published.^[5]

Results and Discussion

The sterically demanding dipyrindylamide ligand precursor Ap*pyH (**1**) (Scheme 2) was synthesized by Pd-catalyzed aryl amination. Treatment of **1** with KH followed by workup afforded the potassium salt of **1** in good yield.



Scheme 2. Syntheses of **1**, **2**, **3a**, and **3b** {Ap*py-H = (6-methylpyridin-2-yl)[6-(2,4,6-triisopropylphenyl)pyridin-2-yl]amine}.

The reaction of **2** with $[\text{YbI}_2(\text{thf})_4]$ ^[7] leads to the bimetallic complex **3a** with a residual iodido ligand at one of the Yb atoms (Scheme 2). The molecular structure of complex **3a** (Figure 1) was investigated by X-ray crystal structure analysis (for crystallographic details please see Table 1) and NMR spectroscopy. The structure of **3a** exhibits two Yb^{II} ions bridged by the amido N atoms of bipyridylamide ligands, which results in a short metal–metal distance

[3.4200(3) Å]. Shorter Yb^{II}–Yb^{II} distances were observed for carbon- and oxygen-bridged dimers.^[8] The Yb–N_{amido} bond lengths are indicative of two symmetric bridges and one nonsymmetrical bridge. The amido N atom of this nonsymmetrical bridge seems to provide the anionic function of the ligand dominantly to the Yb atom that features the additional neutral ligand (thf). In accordance with this the anionic iodido ligand binds the second Yb atom. The bimetallic nature of complex **3a** in solution was confirmed by ^{171}Yb NMR spectroscopy.^[5] A sample of **3a** in C₆D₆ displays two signals at 585.6 (broad, $\nu_{1/2}$ = 92.0 Hz) and 646.6 (sharp, $\nu_{1/2}$ = 8.5 Hz) ppm. The broad signal belongs to Yb2, broadening arises from unresolved ^{171}Yb – ^{127}I scalar coupling. The low-field signal consists of a central singlet and two satellites with an integral intensity of about 7% each. This 14% approximately corresponds to the natural abundance of the ^{171}Yb isotope and was assigned as a doublet arising from $^1J(^{171}\text{Yb}, ^{171}\text{Yb})$ spin–spin coupling with a magnitude of 76.1 Hz. The chemical shift for Yb^{II} amides ranges from $\delta(^{171}\text{Yb})$ = 614 ppm to $\delta(^{171}\text{Yb})$ = 1228 ppm, and the line width associated with ^{171}Yb resonances of these compounds ranges from $\Delta\nu_{1/2}$ = 70 Hz to $\Delta\nu_{1/2}$ = 550 Hz.^[9]

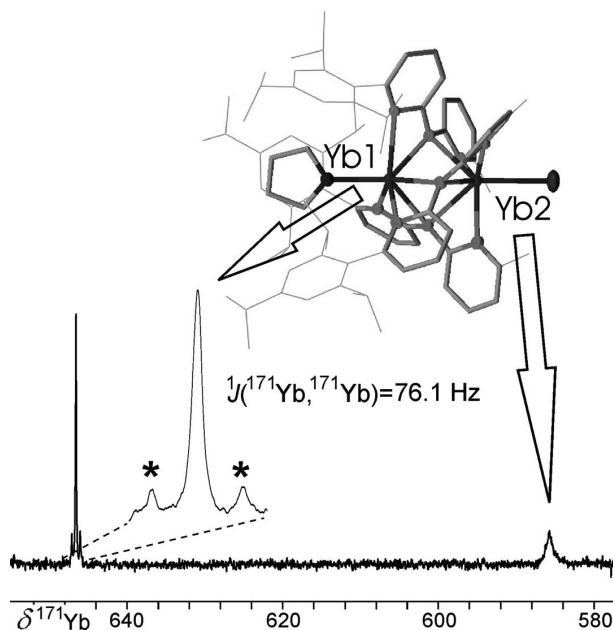
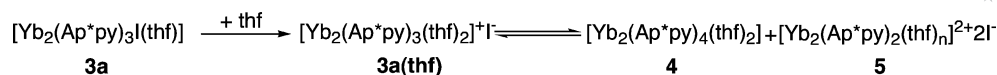
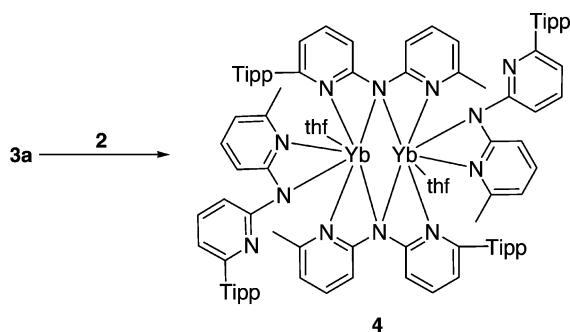


Figure 1. Molecular structure (ORTEP plot for selected atoms with 30% probability) and $^{171}\text{Yb}\{^1\text{H}\}$ NMR spectra (69.96 MHz) of **3a**. Substituents at the pyridine rings are plotted in wire-frame style for clarity. A Yb1–Yb2 distance of 3.4200(3) Å has been observed.

Although complex **3a** is stable in C₆D₆ for days, the ^{171}Yb NMR spectrum in [D₈]THF solution^[5] consists of two already noted resonances (δ = 585.6 and 646.6 ppm) together with a third signal at δ = 679.8 ppm ($\nu_{1/2}$ = 25.5 Hz). In the ^1H NMR spectrum at room temperature there is an additional set of broad signals apart from the set of narrow lines assigned to **3a**. At low temperatures (from 0 °C and lower), the set of broad signals split into two sets (in a ratio of ca. 1:3) of narrow lines where the

Scheme 3. Observed rearrangement reactions of **3a** in THF.

chemical shifts of the major set were completely identical to the shifts found in the ^1H NMR spectrum of binuclear complex **4** (Scheme 3). The ^{171}Yb NMR spectrum of **4** in $[\text{D}_8]\text{THF}$ displayed a signal with a chemical shift ($\delta = 681.9$ ppm) that was very close to the chemical shift of the third signal in the spectrum of **3a** in $[\text{D}_8]\text{THF}$ solution.^[5] Both the ^1H and ^{171}Yb NMR spectra suggest that in THF complex **3a** can dissociate to give the cationic complex **3a(thf)** where the iodido ligand is displaced from the inner coordination sphere by the thf ligand (Scheme 3). The complex **3a(thf)** seems not to be stable and rearranges with the formation of neutral complex **4** and (most likely) dicationic complex **5**. Complex **5** was not detected by NMR spectroscopy because of the low solubility (precipitation was observed). Complex **4** was prepared independently by the reaction of **2** with complex **3a** (Scheme 4).

Scheme 4. Synthesis of **4** [Tipp = 2,4,6-tri(isopropyl)phenyl].

The X-ray crystal structure analysis^[5] of **4** (Figure 2, Table 1) revealed it to be a bimetallic complex in which two bipyridylamide ligands bind both Yb atoms in the double 1,3/1,3-chelating binding mode and the other two in the single 1,3-chelating binding mode, the bridging N atoms and Yb atoms lying in the plane.

The coordination environment around the two ytterbium atoms is identical, hence preventing observation of ^{171}Yb – ^{171}Yb spin-spin coupling. Notably, the distance between the two Yb atoms in **4** [3.8685(11) Å] is longer than in **3a** [3.4200(3) Å], which is probably a result of enhanced steric crowding induced by the additional Ap*py ligand.

A europium analogue of **3a**, compound **3b**, was synthesized by the reaction of **2** with $[\text{EuI}_2(\text{thf})_4]$ (Scheme 2). Crystals of **3b** suitable for X-ray crystal structure analysis (for crystallographic details please see Table 1) were obtained from toluene solution and contain three THF solvate molecules. The molecular structure of **3b** (Figure 3) closely resembles the molecular structure of the ytterbium analog **3a** though with longer Eu–N, Eu–O, and Eu–I bond lengths, which is in accordance with the larger ionic radius

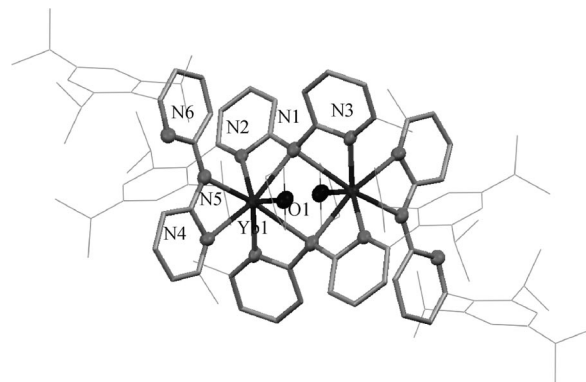


Figure 2. Molecular structure of **4** (ORTEP plot for selected atoms with 30% probability). Substituents at the pyridine rings are plotted in wire-frame style for clarity. Selected bond lengths (Å) and angles (°): Yb1–O1 2.457(6); Yb1–N3 2.462(7), Yb1–N5 2.488(7), Yb1–N1 2.517(8), Yb1–N4 2.586(8), Yb1–N2 2.607(8); N1–Yb1–N2 53.6(2), N3–Yb1–N1 53.0(2), N5–Yb1–N4 52.7(2).

of Eu. The distance Eu1–Eu2 is also in accordance with an increased ionic radius and longer than the Yb1–Yb2 distance in **3a** and amounts to 3.5879(8) Å.

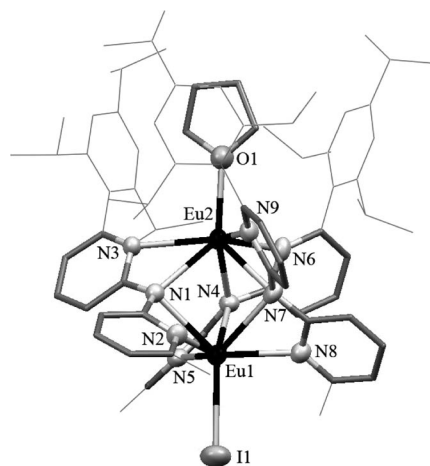


Figure 3. Molecular structure of **3b** (ORTEP plot for selected atoms with 30% probability). Substituents at the pyridine rings are plotted in wire frame style due to clarity. Hydrogen atoms and three THF molecules are omitted. Substituents at the pyridine rings are plotted in the wire frame style for clarity. Selected bond lengths (Å) and angles (°): N1–Eu1 2.711(6), N1–Eu2 2.695(6), N2–Eu1 2.578(7), N3–Eu2 2.751(7), N4–Eu1 2.776(7), N4–Eu2 2.664(7), N5–Eu1 2.576(8), N6–Eu2 2.695(6), N7–Eu1 2.722(7), N7–Eu2 2.727(7), N8–Eu1 2.569(7), N9–Eu2 2.710(7), O1–Eu2 2.525(7), Eu1–I1 3.1671(9); N1–Eu1–N2 51.4(2), N1–Eu2–N3 49.9(2), N7–Eu1–N8 51.3(2), N7–Eu2–N9 50.5(2), N4–Eu1–N5 50.7(2), N4–Eu2–N6 51.1(2), Eu1–N1–Eu2 83.16(18), Eu1–N4–Eu2 82.5(2), Eu1–N7–Eu2 82.4(2).

At room temperature a sample of **3b** gave no ^{151}Eu Mössbauer signal, most likely due to the flexible ligand sphere. The ^{151}Eu Mössbauer spectrum of **3b** at 77 K is pre-

sented in Figure 4 together with a transmission integral fit. The spectrum shows two spectral components, one at an isomer shift (δ) of $-11.9(1)$ mm/s and an experimental line width (Γ) of $6.9(1)$ mm/s and a second signal at $\delta = 0.69(1)$ mm/s and $\Gamma = 3.2(4)$ mm/s. These signals have a ratio of 92:8. The signal at $\delta = 0.69(1)$ mm/s can be attributed to trivalent europium. Most likely this small spectral component arises from partial oxidation of the sample. The main signal at $\delta = -11.9(1)$ mm/s corresponds to divalent europium. The experimental line width of $\Gamma = 6.9(1)$ mm/s, however, is extremely large and results from an overlap of the signals from both crystallographically independent europium sites. A reliable fit with two independent signals could not be obtained.

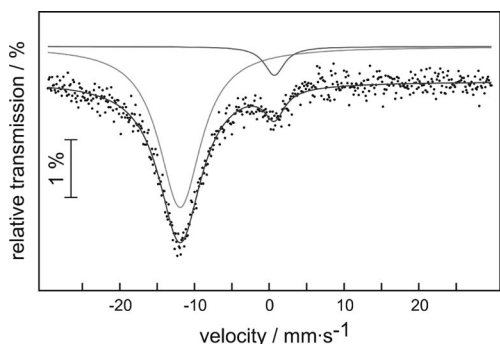
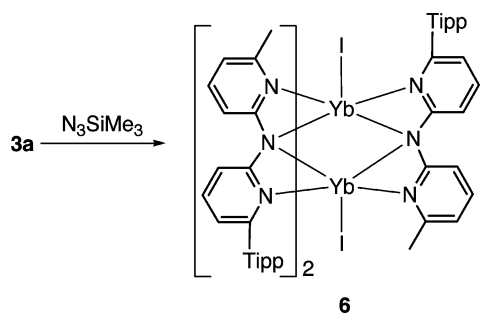


Figure 4. Experimental and simulated ^{151}Eu Mössbauer spectrum of **3b** at 77 K.

The bimetallic complex **3a** features a well-protected coordination site (which is occupied by the thf ligand) by virtue of the 2,4,6-triisopropylphenyl moieties of Ap*py. At the same time the two Yb^{II} ions, which are in close proximity to each other, may cooperate in redox reactions with various substrates leading to the stabilization of complexes with unusual $\text{Yb}-\text{X}$ multiple bonds ($\text{X} = \text{N}-\text{SiMe}_3$ or S). With these ideas in mind we set out to explore the redox chemistry of **3a**. The reaction of the bimetallic complex **3a** with azidotrimethylsilane, however, did not result in the isolation of a complex with a terminal imido ligand, but the bimetallic complex **6** with two iodido ligands each at both Yb atoms was obtained in 31% yield (Scheme 5). An imido species if formed in this reaction, seems not to be stable and a rearrangement with the formation of **6** is observed.



Scheme 5. Synthesis of **6**, yield 31% [Tipp = 2,4,6-tri(isopropyl)phenyl].

Since the paramagnetic nature of **6** prevents its detailed structural characterization by NMR spectroscopy, X-ray crystal structure analysis was performed. Crystallographic details are listed in Table 1. The two Yb atoms in complex **6** (Figure 5) are bridged by three bipyridylamide ligands. The $\text{Yb1}-\text{N}_{\text{amido}}$ and $\text{Yb1}-\text{N}_{\text{pyridine}}$ bond lengths are longer than the $\text{Yb2}-\text{N}_{\text{amido}}$ and $\text{Yb2}-\text{N}_{\text{pyridine}}$ bond lengths. This indicates that the formal oxidation states II and III could be assigned to Yb1 and Yb2, respectively. In accordance with this assignment the bond length $\text{Yb1}-\text{I1}$ [$3.0333(8)$ Å] is longer than the bond length $\text{Yb2}-\text{I2}$ [$2.9425(7)$ Å]. The distance $\text{Yb1}-\text{Yb2}$ [$3.5179(6)$ Å] is longer than the corresponding metal–metal distance in complex **3a**. Similarly the reaction of the bimetallic complex **3a** with sulfur did not result in the isolation of a complex with a terminal sulfido ligand, a class of compounds unknown for lanthanoids. However, in contrast to the reaction with azidotrimethylsilane the bimetallic complex **7** with two Yb^{III} ions was formed (Scheme 6). We suggest that the same explanation can be invoked to rationalize the formation of **7** as was proposed for the formation of complex **6**.

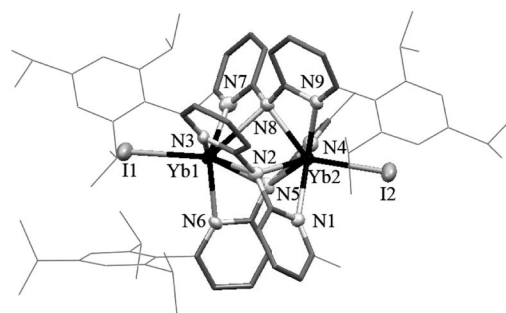
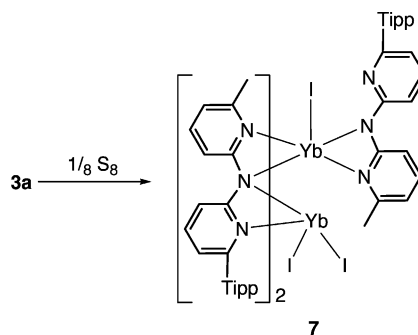


Figure 5. Molecular structure of **6** (ORTEF plot for selected atoms with 30% probability). Hydrogen atoms and one toluene molecule are omitted. Substituents at the pyridine rings are plotted in the wire-frame style for clarity. Selected bond lengths (Å) and angles ($^\circ$): $\text{N1}-\text{Yb2}$ 2.431(7), $\text{N2}-\text{Yb2}$ 2.453(6), $\text{N2}-\text{Yb1}$ 2.615(7), $\text{N3}-\text{Yb1}$ 2.512(7), $\text{N4}-\text{Yb2}$ 2.363(8), $\text{N5}-\text{Yb2}$ 2.371(7), $\text{N5}-\text{Yb1}$ 2.622(7), $\text{N6}-\text{Yb1}$ 2.531(7), $\text{N7}-\text{Yb1}$ 2.469(8), $\text{N8}-\text{Yb1}$ 2.788(7), $\text{N8}-\text{Yb2}$ 2.387(7), $\text{N9}-\text{Yb2}$ 2.450(7), $\text{Yb1}-\text{I1}$ 3.0333(8), $\text{Yb2}-\text{I2}$ 2.9425(7); $\text{N1}-\text{Yb2}-\text{N2}$ 55.5(2), $\text{N5}-\text{Yb2}-\text{N4}$ 56.8(2), $\text{N8}-\text{Yb2}-\text{N9}$ 56.6(2), $\text{N2}-\text{Yb1}-\text{N3}$ 53.8(2), $\text{N5}-\text{Yb1}-\text{N6}$ 52.7(2), $\text{N7}-\text{Yb1}-\text{N8}$ 50.7(2), $\text{Yb1}-\text{N2}-\text{Yb2}$ 87.8(2), $\text{Yb1}-\text{N5}-\text{Yb2}$ 89.5(2), $\text{Yb1}-\text{N8}-\text{Yb2}$ 85.3(2).



Scheme 6. Synthesis of **7**, yield 22% [Tipp = 2,4,6-tri(isopropyl)phenyl].

The X-ray crystal structure analysis of **7** (Figure 6, Table 1) revealed it to be a bimetallic complex in which two Ap*py ligands act as tridentate bridging ligands towards both Yb atoms and one of them acts as a terminal bidentate amidopyridine ligand towards Yb2. Two ytterbium atoms and two amido atoms N5 and N8 form an almost planar arrangement. Examination of Yb–N_{amido} and Yb–N_{pyridine} bond lengths suggests that N2 and N7 seem to provide the anionic function of the ligands to Yb2, whereas N5 provides the anionic function to Yb1. Noteworthy, the distance Yb1–Yb2 [3.8052(6) Å] is significantly longer than the corresponding metal–metal distance in the starting complex **3a** and significantly longer than in the mixed valence compound **6**. Since all three compounds do have the same coordination environment considering the N ligands the increased charge might be an explanation for the elongation trend.

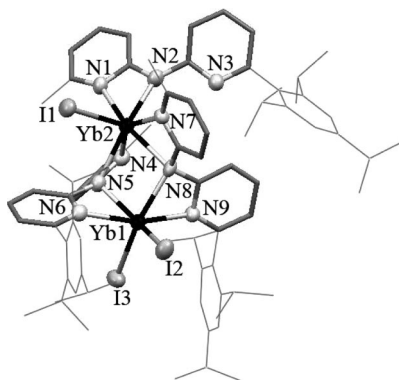
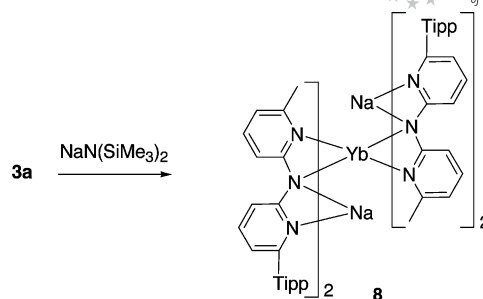


Figure 6. Molecular structure of **7** (ORTEP plot for selected atoms with 30% probability). Hydrogen atoms, five benzene molecules, and one toluene molecule are omitted. Substituents at the pyridine rings are plotted in the wire-frame style for clarity. Selected bond lengths (Å) and angles (°): N1–Yb2 2.384(6), N2–Yb2 2.294(6), N4–Yb2 2.437(6), N5–Yb2 2.482(6), N5–Yb1 2.367(6), N6–Yb1 2.405(6), N7–Yb2 2.383(6), N8–Yb2 2.471(6), N8–Yb1 2.409(6), N9–Yb1 2.375(6), Yb1–I2 2.8462(7), Yb1–I3 2.8742(7), Yb2–I1 2.9511(6); N1–Yb2–N2 57.1(2), N4–Yb2–N5 54.2(2), N7–Yb2–N8 56.4(2), N5–Yb1–N6 57.0(2), N8–Yb1–N9 57.69(19), N5–Yb2–N8 75.1(2), N5–Yb1–N8 78.4(2).

Attempted substitution of the iodido ligand in **3a** with the bis(trimethylsilyl)amido ligand by treating **3a** with NaN(SiMe₃)₂ resulted in the formation of homoleptic “ate” complex **8** (Scheme 7) which was characterized by ¹H and ¹³C NMR spectroscopy as well as by X-ray crystal structure analysis.

The molecular structure of complex **8** (Figure 7, Table 1) exhibits an eight-coordinate Yb^{II} ion with four Ap*py ligands coordinated in bidentate fashion with the less sterically hindered 6-methylpyridin-2-amido functions. The unused 6-(2,4,6-triisopropylphenyl)pyridine functions together with the amido nitrogen atoms now bind two sodium atoms. Noteworthy in particular is the linear arrangement of the three metal atoms. A plethora of linear trimetallic complexes with four dipyriddydamido ligands are known for late transition metals.^[10] However, in **8** each of the Ap*py ligands bind only two metal atoms, whereas in the related



Scheme 7. Synthesis of **8**, yield 28% [Tipp = 2,4,6-tri(isopropyl)phenyl].

structurally characterized transition-metal complexes each of the dipyriddydamide ligands binds all three metal atoms. Another noteworthy feature is the heterometallic nature of **8** since complexes of this type with two different metals are rare: the realm of dipyriddydamido complexes with a trimetallic backbone is embellished, for instance, by a heterometallic Co–Pd–Co complex prepared by Peng and co-workers.^[11]

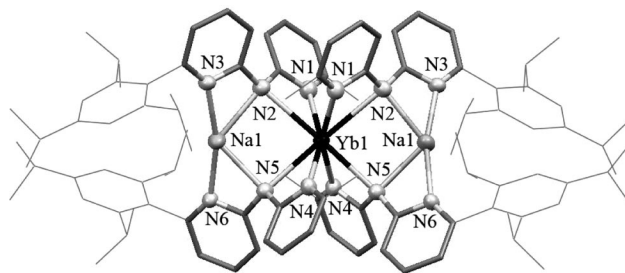
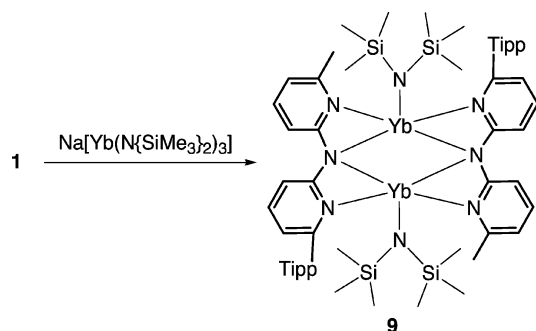
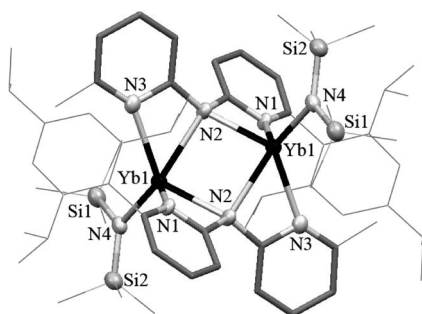


Figure 7. Molecular structure of **8** (ORTEP plot for selected atoms with 30% probability). Hydrogen atoms and three benzene molecules are omitted. Substituents at the pyridine rings are plotted in the wire-frame style for clarity. Selected bond lengths (Å) and angles (°): N1–Yb1 2.557(5), N2–Yb1 2.789(5), N4–Yb1 2.563(5), N5–Yb1 2.644(5), N5–Na1 2.423(5), N6–Na1 2.304(5), N2–Na1 2.422(6), N3–Na1 2.297(5); N1–Yb1–N2 50.48(15), N4–Yb1–N5 51.92(15), N5–Na1–N6 58.33(17), N2–Na1–N3 58.50(17).

Thus, the outcome of the reaction between **3a** and NaN(SiMe₃)₂ might be explained in terms of low steric demand of the 6-methylpyridine function in **1** leading to rearrangement with formation of highly nitrogen-coordinated species.

The mixed silylamide bipyridylamide complex **9** was prepared in 40% yield in the form of black crystals by treating one equivalent of ligand **1** with one equivalent of Na[Yb(N{SiMe₃}₂)₃]^[12] (Scheme 8).

Complex **9** was characterized by ¹H NMR spectroscopy from which the ratio silylamide/bipyridylamide can be deduced. However, the precise molecular geometry was established by X-ray crystal structure analysis (Figure 8, Table 1) and revealed it to be a bimetallic complex. The structural model of complex **9** features an inversion center with two crystallographically equivalent Yb atoms. These two Yb atoms are separated by 3.6547(7) Å and are bridged by two Ap*py ligands.

Scheme 8. Synthesis of **9** [Tipp = 2,4,6-tri(isopropyl)phenyl].Figure 8. Molecular structure of **9** (ORTEP plot for selected atoms with 30% probability). Hydrogen atoms are omitted and substituents at the pyridine rings are plotted in the wire-frame style for clarity. Selected bond lengths (Å) and angles (°): N1–Yb1 2.485(5), N2–Yb1 2.550(5), N2–Yb1' 2.547(5), N3–Yb1 2.497(5), N4–Yb1 2.304(5); N1–Yb1–N2 54.60(15), N2–Yb1–N3 53.99(16).

Conclusions

First, the reaction of the potassium salt of sterically demanding dipyridylamine Ap*pyH with $[\text{YbI}_2(\text{thf})_4]$ or with $[\text{EuI}_2(\text{thf})_4]$ afforded novel dinuclear Yb^{II} and Eu^{II} complexes that were structurally characterized. In these complexes the metal centers are in close proximity and in a chemically different environment. This allowed us to observe ^{171}Yb – ^{171}Yb spin–spin coupling in solution. Investigation of the corresponding Eu complex by Mössbauer

spectroscopy did not allow the observation of two Eu^{II} signals but an unexceptional broad signal for both Eu atoms of the bimetallic complex.

Second, the Ap*py ligand is highly flexible in its coordination behavior which could be concluded from the isolation and structural characterization of a variety of bimetallic Yb complexes including a heterobimetallic trimeric molecular wire-type compound.

Experimental Section

General Procedures: All reactions and manipulations with air-sensitive compounds were performed with exclusion of oxygen and moisture in Schlenk-type glassware on a dual manifold Schlenk line or in a nitrogen-filled glove box (mBraun 120-G) with a high-capacity recirculator (<0.1 ppm O_2). Nonhalogenated solvents were dried by distillation from sodium wire/benzophenone ketyl. Deuterated solvents were obtained from Cambridge Isotope Laboratories and were dried and distilled prior to use. The 2-amino-6-methylpyridine (Aldrich) was purified by crystallization from pentane prior to use. $\text{EuI}_2(\text{thf})_4$ was made by recrystallizing EuI_2 (STREM) in THF. All other chemicals were purchased from commercial vendors and used without further purification. NMR spectra were recorded with a Bruker ARX 250 MHz, ARX 500 MHz, or Varian INOVA 400 MHz. Chemical shifts are given in ppm; they were measured at ambient temperature and are referenced to internal TMS for ^1H and ^{13}C . The ^{171}Yb NMR spectra were recorded by using a single-pulse sequence with pulse: approx. 30° , relaxation delay, 1 s, digital FID resolution: 0.3–0.5 Hz before zero filling and with proton decoupling during acquisition. The suitable signal-to-noise ratio was reached after 2–4 h. The chemical shifts are given relative to 0.171 M $[\text{Yb}(\eta^5\text{-C}_5\text{Me}_5)(\text{thf})_2]$ in THF [$\delta(^{171}\text{Yb}) = 0$ ppm for $\Xi(^{171}\text{Yb}) = 17.499306$ MHz]. Elemental analyses (CHN) were determined with a Vario EL III instrument. Melting points were determined with a Stuart SMP3 apparatus and are uncorrected. X-ray crystal structure analyses were performed with a STOE-IPDS II equipped with an Oxford Cryostream low-temperature unit. Structure solution and refinement was accomplished using SIR97,^[13] SHELXL97,^[14] and WinGX.^[15] Crystallographic details are summarized in Table 1.

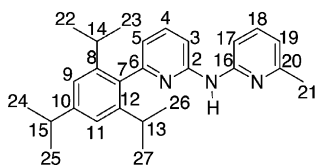
CCDC-642879 (for **3a**), -705292 (for **3b**) -642880 (for **4**) -705293 (for **6**), -705294 (for **7**), -705295 (for **8**), and -705296 (for **9**) contain

Table 1. Crystallographic details.

Compound	3a	3b	4	6	7	8	9
Crystal system	triclinic	triclinic	triclinic	triclinic	triclinic	monoclinic	triclinic
Space group	$P\bar{1}$	$P\bar{1}$	$P\bar{1}$	$P\bar{1}$	$P\bar{1}$	$C2/c$	$P\bar{1}$
<i>a</i> [Å]	13.3350(5)	13.3710(13)	14.2870(12)	16.8872(8)	14.7390(13)	24.847(5)	11.8050(9)
<i>b</i> [Å]	15.8580(6)	15.9180(15)	14.3730(10)	17.1111(8)	17.8160(15)	16.294(5)	12.2370(9)
<i>c</i> [Å]	22.9500(9)	23.045(2)	16.8380(14)	19.0067(9)	23.3260(19)	32.932(5)	12.9310(9)
α [°]	102.371(3)	102.303(8)	114.563(6)	85.362(4)	74.554(7)		71.914(5)
β [°]	91.499(3)	91.434(8)	93.070(6)	69.156(4)	89.109(7)	108.800(5)	74.443(5)
γ [°]	107.584(3)	107.301(8)	109.525(6)	65.729(4)	65.568(6)		81.613(6)
<i>V</i> [Å ³]	4497.4(3)	4554.8(8)	2888.2(4)	4665.2(4)	5343.9(8)	12621(5)	1706.6(2)
<i>Z</i>	2	2	2	2	2	4	2
<i>F</i> (000)	1964	1932	1140	1746	2330	4336	736
ρ (calcd.) [g cm ⁻³]	1.42	1.37	1.26	1.25	1.45	1.09	1.40
μ [mm ⁻¹]	2.5	1.8	1.7	2.7	2.7	0.8	2.8
<i>T</i> [K]	191(2)	193(2)	191(2)	193(2)	193(2)	191(2)	173(2)
2θ range [°]	2.78–52.20	2.77–52.19	2.78–48.82	2.83–52.27	2.62–46.38	2.61–52.22	3.41–52.03
<i>R</i> ₁ , <i>wR</i> ₂ [<i>I</i> > 2σ(<i>I</i>)]	0.0336, 0.0785	0.0664, 0.1297	0.0654, 0.1201	0.0770, 0.2518	0.0440, 0.0997	0.0699, 0.1889	0.0409, 0.0818
<i>R</i> ₁ , <i>wR</i> ₂ (all data)	0.0488, 0.0825	0.1469, 0.1537	0.1377, 0.1385	0.0938, 0.2713	0.0621, 0.1060	0.0868, 0.2018	0.0645, 0.0864

the supplementary crystallographic data for this publication. These data can be obtained free of charge at www.ccdc.cam.ac.uk/conts/retrieving.html (or from the Cambridge Crystallographic Data Centre, 12 Union Road, Cambridge CB2 1EZ, UK; Fax: + 44-1223-336-033; E-mail: deposit@ccdc.cam.ac.uk).

Synthesis of (Ap*py)H (1): {(Ap*py)H = (6-methylpyridin-2-yl)-[6-(2,4,6-triisopropylphenyl)pyridin-2-yl]amine; for the atom numbering of Ap*pyH (1) and complexes thereof see formula} A mixture of 2-bromo-6-(2,4,6-triisopropylphenyl)pyridine (10.8 g, 30.0 mmol), 2-amino-6-methylpyridine (4.00 g, 37.0 mmol), and sodium *tert*-butoxide (3.00 g, 31.3 mmol) was dissolved in toluene (150 mL). Then a solution of 1,3-bis(diphenylphosphanyl)propane (1.00 g, 2.42 mmol) and tris(dibenzylideneacetone)dipalladium(0) (1.00 g, 1.09 mmol) in THF (30 mL) was added and the resulting reaction mixture was stirred at 90 °C for 16 h. After cooling to room temperature, water (20 mL) was added, the organic phase was separated and the aqueous phase was washed with diethyl ether (3 × 20 mL). The combined organic phases were washed with a saturated sodium chloride solution and dried with sodium sulfate. The volatiles were removed in a vacuum leaving an orange-brown residue that was purified by column chromatography on a silica gel using dichloromethane as eluent. Removal of dichloromethane and washing with cold pentane afforded a beige solid; yield 9.50 g (82%); m.p. 159 °C. C₂₆H₃₃N₃ (387.56): calcd. C 80.58, H 8.58, N 10.84; found C 80.56, H 8.56, N 10.21. ¹H NMR (400 MHz, [D₈]-THF): δ = 1.09 (d, ³J = 6.8 Hz, 6 H, 22-H, 23-H/26-H, 27-H), 1.10 (d, ³J = 6.8 Hz, 6 H, 22-H, 23-H/26-H, 27-H), 1.28 (d, ³J = 7.2 Hz, 6 H, 24-H, 25-H), 2.38 (s, 3 H, 21-H), 2.70 (sept, ³J = 6.8 Hz, 2 H, 13-H, 14-H), 2.91 (sept, ³J = 7.2 Hz, 1 H, 15-H), 6.59 (d, ³J = 7.2 Hz, 1 H, 19-H), 6.69 (dd, ³J = 7.2, ⁴J = 0.4 Hz, 1 H, 5-H), 7.06 (s, 2 H, 9-H, 11-H), 7.35 (dd, ³J = 7.2, ³J = 8.0 Hz, 1 H, 18-H), 7.52 (d, ³J = 8.0 Hz, 1 H, 17-H), 7.57 (dd, ³J = 7.2, ³J = 8.4 Hz, 1 H, 4-H), 7.66 (d, ³J = 8.4 Hz, 1 H, 3-H), 8.8 (br., 1 H, N-H) ppm. ¹³C NMR (100.5 MHz, [D₈]-THF): δ = 24.4 (C-21), 24.4 (C-22, C-23/C-26, C-27), 24.5 (C-22, C-23/C-26, C-27), 24.6 (C-24, C-25), 31.1 (C-13, C-14), 35.3 (C-15), 109.3 (C-17), 110.2 (C-3), 115.2 (C-19), 117.4 (C-5), 120.9 (C-9, C-11), 137.6 (C-4), 138.1 (C-7, C-18), 147.0 (C-8, C-12), 148.8 (C-10), 155.1 (C-16), 155.3 (C-2), 156.8 (C-20), 158.7 (C-6) ppm.



Synthesis of K(Ap*py)·THF (2): To a mixture of **1** (3.00 g, 7.74 mmol) and potassium hydride (0.70 g, 17.5 mmol) was slowly added diethyl ether (150 mL) at 0 °C. The reaction mixture was stirred at ambient temperature for 16 h. The volatiles were removed in a vacuum and the product was extracted twice with THF and the solution was filtered. The solvent was removed under reduced pressure and the resulting beige solid was washed with hexane; yield 3.00 g (77.9%); m.p. 110 °C. C₂₆H₃₂KN₃·C₄H₈O (497.76): calcd. C 72.39, H 8.10, N 8.44; found C 72.17, H 8.87, N 8.43. ¹H NMR (400 MHz, [D₈]-THF): δ = 1.06 (d, ³J = 6.8 Hz, 6 H, 22-H, 23-H/26-H, 27-H), 1.07 (d, ³J = 6.8 Hz, 6 H, 22-H, 23-H/26-H, 27-H), 1.24 (d, ³J = 7.2 Hz, 6 H, 24-H, 25-H), 1.71 (br., 4 H, β-CH₂, THF), 2.15 (s, 3 H, 21-H), 2.86 (sept, ³J = 7.2 Hz, 1 H, 15-H), 2.90 (sept, ³J = 6.8 Hz, 2 H, 13-H, 14-H), 3.57 (br., 4 H, α-CH₂, THF), 6.01 (d, ³J = 6.9 Hz, 1 H, 19-H), 6.05 (d, ³J = 7.0 Hz, 1 H, 5-H), 6.74 (d, ³J = 8.5 Hz, 1 H, 3-H), 6.96 (dd, ³J = 6.9, ³J = 8.5 Hz, 1 H, 18-H), 6.97 (s, 2 H, 9-H, 11-H), 7.07 (dd, ³J = 7.0, ³J = 8.5 Hz,

1 H, 4-H), 7.40 (d, ³J = 8.5 Hz, 1 H, 17-H) ppm. ¹³C NMR (100.5 MHz, [D₈]-THF): δ = 24.6 (C-21, C-24, C-25), 24.8 (C-22, C-23/C-26, C-27), 25.0 (C-22, C-23/C-26, C-27), 26.3 (β-CH₂, THF), 30.8 (C-13, C-14), 35.3 (C-15), 68.2 (α-CH₂, THF), 108.2 (C-19), 110.5 (C-17), 111.0 (C-5), 113.2 (C-3), 120.7 (C-9, C-11), 135.5 (C-4), 136.6 (C-18), 140.3 (C-7), 146.9 (C-8, C-12), 147.6 (C-10), 156.4 (C-20), 158.5 (C-6), 166.8 (C-16), 167.0 (C-2) ppm.

Synthesis of Yb₂I(Ap*py)₃(THF) (3a): In a glove box, [YbI₂(thf)₄] (2.13 g, 2.98 mmol) and **2** (1.90 g, 3.82 mmol) were combined in a flask and THF (100 mL) was added at 0 °C. The resulting dark red reaction mixture was stirred at room temperature for 16 h. After separation of the solution from the precipitated potassium iodide by filtration, the solvent was removed under reduced pressure. The resulting solid was dissolved in toluene (100 mL) and again filtered. The filtrate was reduced to dryness, and a dark red-black product was obtained. Crystals of **3a** were grown from a concentrated toluene solution; yield 2.06 g (72%); m.p. 190 °C. C₈₂H₁₀₄IN₉OYb₂·3C₄H₈O (1921.06): calcd. C 58.77, H 6.72, N 6.56; found C 58.77, H 6.67, N 6.93. ¹H NMR (250 MHz, C₆D₆, 323 K): δ = 0.67–1.24 (m, ³J = 6.7 Hz, 54 H, 22-H, 23-H, 24-H, 25-H, 26-H, 27-H), 1.43 (br., 4 H, β-CH₂, thf), 2.38 (sept, ³J = 6.9 Hz, 3 H, 15-H), 2.60 (sept, ³J = 7.0 Hz, 3 H, 14-H), 2.66 (s, 9 H, 21-H), 2.78 (sept, ³J = 6.7 Hz, 3 H, 13-H), 3.53 (br., 4 H, α-CH₂, thf), 6.00 (d, ³J = 6.7 Hz, 3 H, 19-H), 6.16 (d, ³J = 6.6 Hz, 3 H, H⁵), 6.83–7.16 (m, 18 H, 3-H, 4-H, 9-H, 11-H, 17-H, 18-H) ppm. ¹³C NMR (62.9 MHz, C₆D₆): δ = 24.0 (s, C-22, C-23, C-26, C-27), 24.1 (s, C-22, C-23, C-26, C-27), 24.2 (s, C-22, C-23, C-26, C-27), 24.3 (s, C-22, C-23, C-26, C-27), 26.1 (s, β-CH₂, thf), 26.8 (s, C-24, C-25), 27.1 (s, C-24, C-25), 29.8 (s, C-13, C-14), 30.0 (s, C-13, C-14), 34.6 (s, C-15), 67.7 (s, α-CH₂, thf), 109.5 (s, C-19), 113.4 (s, C-17), 114.5 (s, C-5), 116.2 (s, C-3), 121.0 (s, C-9, C-11), 135.8 (s, C-4), 137.5 (s, C-7, C-18), 137.6 (s, C-7, C-18), 146.9 (s, C-8, C-12), 147.1 (s, C-8, C-12), 148.5 (s, C-10), 156.8 (s, C-2, C-16), 157.4 (s, C-2, C-16), 164.2 (s, C-20), 169.1 (s, C-6) ppm. ¹⁷¹Yb NMR (70 MHz, C₄H₈O): δ = 646.6 [s, ¹J(¹⁷¹Yb, ¹⁷¹Yb) = 76.1 Hz, Yb-thf], 585.6 (br., Yb-I) ppm.

Synthesis of Yb₂(Ap*py)₄(THF)₂ (4): In a NMR tube a solution of **3a** (0.250 g, 0.147 mmol) in [D₈]-THF (0.5 mL) was combined with **2** (0.062 g, 0.127 mmol) and the black solution was filtered. The solution was kept at –30 °C for 48 h to afford deep red nearly black crystals of **4**; yield (0.075 g, 29%). C₁₁₂H₁₄₄N₁₂O₂Yb₂ (2036.50): calcd. C 66.05, H 7.13, N 8.25; found C 66.23, H 7.16, N 8.03. ¹H NMR (500.13 MHz, [D₈]-THF): δ = 1.08 (d, ³J = 6.9 Hz, 24 H, 22-H, 26-H), 1.11 (d, ³J = 6.9 Hz, 24 H, 23-H, 27-H), 1.26 (d, ³J = 6.9 Hz, 24 H, 24-H, 25-H), 2.05 (s, 12 H, 21-H), 2.86 (m, 12 H, 13-H, 14-H, 15-H), 6.04 (d, ³J = 4.7 Hz, 4 H, 3-H), 6.28 (d, ³J = 5.7 Hz, 4 H, 17-H), 6.68 (d, ³J = 6.2 Hz, 4 H, 19-H), 7.00 (s, 8 H, 9-H, 11-H), 7.08 (dd, ³J = 4.7, ³J = 8.0 Hz, 4 H, 4-H), 7.23 (dd, ³J = 5.7, ³J = 6.2 Hz, 4 H, 18-H), 7.74 (d, ³J = 8.0 Hz, 4 H, 5-H) ppm. ¹³C NMR (125.8 MHz, [D₈]-THF): δ = 24.0 (C-21), 25.1, 25.3, 25.4 (C-22, C-23, C-24, C-25, C-26, C-27), 31.5 (C-13, C-14), 35.9 (C-15), 109.9 (C-3), 110.6 (C-5), 113.6 (C-17), 114.8 (C-19), 121.2 (C-9, C-11), 136.2 (C-18), 138.3 (C-4), 140.3 (C-20), 147.4 (C-8, C-12), 148.5 (C-7), 155.4 (C-6), 158.9 (C-10), 165.0 (C-2/C-16), 166.9 (C-2/C-16) ppm. ¹⁷¹Yb NMR (69.96 MHz, [D₈]-THF): δ = 679.8 ppm.

Synthesis of Eu₂I(Ap*py)₃(THF)₃(THF) (3b): To a mixture of EuI₂ (0.812 g, 2.0 mmol) and **2** (1.40 g, 2.82 mmol) was added THF (100 mL) at 0 °C. The resulting orange reaction mixture was stirred at room temperature for 16 h. Potassium iodide was removed by filtration and the solvent was removed under reduced pressure. The resulting solid was dissolved in toluene (100 mL) and again filtered. The filtrate was concentrated to a small volume and cooled to

–30 °C affording crystals of **3b**; yield 1.65 g (88%); m.p. 182 °C. C₈₂H₁₀₄Eu₂IN₉O·3C₄H₈O (1878.87): calcd. C 60.09, H 6.87, N 6.71; found C 59.85, H 6.74, N 7.13.

¹⁵¹Eu Mössbauer Spectroscopy of Eu₂I(Ap*py)₃(THF)·3THF (3b**):** The 21.53 keV transition of ¹⁵¹Eu with an activity of 130 MBq (2% of the total activity of a ¹⁵¹Sm:EuF₃ source) was used for the Mössbauer spectroscopic investigation of **3b** at room temperature and 77 K. The sample was placed within a sealed glass container at a thickness corresponding to about 10 mg Eu/cm².

Synthesis of Yb₂I₂(Ap*py)₃·2(C₇H₈) (6**):** A solution of **4** (0.576 g, 0.30 mmol) and N₃SiMe₃ (0.1 mL, 0.76 mmol) in toluene (40 mL) was stirred at room temperature for 15 h. The reaction mixture was filtered, concentrated in a vacuum and cooled to –20 °C. After 24 h dark-red crystals of **6** were isolated by filtration affording 0.180 g (31%); m.p. 227 °C. C₇₈H₉₆I₂N₉Yb₂·2(C₇H₈) (1943.82): calcd. C 56.85, H 5.81, N 6.49; found C 56.89, H 5.61, N 6.60.

Synthesis of Yb₂I₃(Ap*py)₃·(C₆D₆) (7**):** In a NMR tube a sample of **4** (0.100 g, 0.052 mmol) was dissolved in C₆D₆ (1 mL) and the ¹H NMR spectrum was recorded. Then sulfur (0.011 g, 0.344 mmol) was added and the red solution was filtered. Keeping the solution at ambient temperature for 2 d afforded red crystals of **7** (0.022 g, 22%); m.p. 279 °C. C₇₈H₉₆I₃N₉Yb₂·(C₆D₆) (1970.59): calcd. C 51.20, H 5.52, N 6.40; found C 51.35, H 4.95, N 6.06.

Synthesis of Na₂Yb(Ap*py)₄·(C₇D₈) (8**):** In a NMR tube a sample of **4** (0.100 g, 0.052 mmol) was dissolved in [D₈]toluene (0.5 mL) and the ¹H NMR spectrum was recorded. Then NaN(SiMe₃)₂ (0.037 g, 0.20 mmol) was added and the tube was heated at 100 °C for 2 h. The dark black-brown reaction mixture was filtered and the solution was kept at room temperature for 48 h to yield black crystals of **8** (0.027 g, 28%). C₁₀₄H₁₂₈N₁₂Na₂Yb·(C₇D₈) (1865.41): calcd. C 71.47, H 7.78, N 9.01; found C 71.82, H 7.22, N 9.15. ¹H NMR (250 MHz, C₇D₈): δ = 0.96 (d, ³J = 7.1 Hz, 24 H, 22-H, 23-H/26-H, 27-H), 1.09 (d, ³J = 6.8 Hz, 24 H, 22-H, 23-H/26-H, 27-H), 1.24 (d, ³J = 6.9 Hz, 24 H, 24-H, 25-H), 2.03 (s, 12 H, 21-H), 2.80 (m, 12 H, 13-H, 14-H, 15-H), 6.08 (d, J = 6.8 Hz, 4 H, 19-H), 6.35 (d, ³J = 6.9 Hz, 4 H, 5-H), 6.78 (d, ³J = 8.3 Hz, 4 H, 3-H), 6.98–7.14 (m, 20 H, 4-H, 9-H, 11-H, 17-H, 18-H) ppm. ¹³C NMR (62.9 MHz, C₇D₈): δ = 24.2–25.9 (C-21, C-22, C-23, C-24, C-25, C-26, C-27), 30.4 (C-13/C-14), 30.5 (C-13/C-14), 34.9 (C-15), 108.1 (C-3/C-5/C-17/C-19), 111.3 (C-3/C-5/C-17/C-19), 112.0 (C-3/C-5/C-17/C-19), 114.8 (C-3/C-5/C-17/C-19), 120.8 (C-9/C-11), 121.0 (C-9/C-11), 146.7 (C-2/C-6/C-8/C-10/C-12/C-16/C-20), 148.8 (C-2/C-6/C-8/C-10/C-12/C-16/C-20), 155.9 (C-2/C-6/C-8/C-10/C-12/C-16/C-20), 158.3 (C-2/C-6/C-8/C-10/C-12/C-16/C-20), 166.0 (C-2/C-6/C-8/C-10/C-12/C-16/C-20), 166.1 (C-2/C-6/C-8/C-10/C-12/C-16/C-20) ppm.

Synthesis of [Yb₂(Ap*py)₂{N(SiMe₃)₂}]·(C₆D₆) (9**):** In a NMR tube a mixture of NaYb[N(SiMe₃)₂]₃(THF) (0.075 g, 0.100 mmol) and **1** (0.039 g, 0.100 mmol) was dissolved in C₆D₆ (0.5 mL) and the ¹H NMR spectrum was recorded. Then the dark-black reaction mixture was filtered and the solution was kept at room temperature for 12 h to yield black crystals of **9** (0.030 g, 40%). C₆₄H₁₀₀N₈Si₄Yb₂·C₆D₆ (1524.10): calcd. C 55.16, H 7.41, N 7.35; found C 55.19, H 7.17, N 7.36. ¹H NMR (250 MHz, C₆D₆): δ = 0.18 (36 H, SiMe₃), 0.92–1.07 (m, 18 H, 22-H, 23-H, 24-H, 25-H, 26-H, 27-H), 2.24 (s, 3 H, 21-H), 2.60 (m, 3 H, 13-H, 14-H, 15-H), 5.94 (br., 1 H, 19-H), 6.27 (br., 1 H, 5-H), 6.39 (br., 1 H, 3-H), 6.74–7.25 (m, 5 H, 4-H, 9-H, 11-H, 17-H, 18-H) ppm. ¹³C NMR (62.9 MHz, C₆D₆): δ = 5.4 (SiMe₃), 23.4 (C-21), 24.1 (C-22, C-23, C-26, C-27), 25.7 (C-24, C-25), 30.1 (C-13, C-14), 34.5 (C-15), 107.5 (C-19), 111.3 (C-17), 111.6 (C-5), 116.0 (C-3), 120.5 (C-9, C-11), 136.8 (C-7), 137.3 (C-9), 138.7 (C-18), 146.0 (C-8, C-12), 148.8

(C-10), 155.4 (C-20), 158.7 (C-6), 165.1 (C-16), 165.7 (C-2) ppm. ²⁹Si NMR (49.69 MHz, C₆D₆): δ = 14.0 ppm. ¹⁷¹Yb NMR (43.77 MHz, C₆D₆): δ = 503.4 ppm.

Acknowledgments

We thank the Deutsche Forschungsgemeinschaft (DFG) (SPP 1166 “Lanthanide Specific Functionalities in Molecules and Materials”) for financial support.

- [1] Review articles on aminopyridinato ligands: R. Kempe, *Eur. J. Inorg. Chem.* **2003**, 791–803; R. Kempe, H. Noos, T. Irrgang, *J. Organomet. Chem.* **2002**, 647, 12–20.
- [2] a) N. M. Scott, T. Schareina, O. Tok, R. Kempe, *Eur. J. Inorg. Chem.* **2004**, 3297–3304; b) N. M. Scott, R. Kempe, *Eur. J. Inorg. Chem.* **2005**, 1319–1324; c) W. P. Kretschmer, A. Meetsma, B. Hessen, N. M. Scott, S. Qayyum, R. Kempe, *Z. Anorg. Allg. Chem.* **2006**, 632, 1936–1938; d) W. P. Kretschmer, A. Meetsma, B. Hessen, T. Schmalz, S. Qayyum, R. Kempe, *Chem. Eur. J.* **2006**, 12, 8969–8978; e) W. P. Kretschmer, B. Hessen, A. Noor, N. M. Scott, R. Kempe, *J. Organomet. Chem.* **2007**, 692, 4569–4579; f) S. M. Guillaume, M. Schappacher, N. M. Scott, R. Kempe, *J. Polym. Sci., Part A: Polym. Chem.* **2007**, 45, 3611–3619; g) A. M. Dietel, O. Tok, R. Kempe, *Eur. J. Inorg. Chem.* **2007**, 4583–4586; h) S. Qayyum, K. Haberland, C. M. Forsyth, P. C. Junk, G. B. Deacon, R. Kempe, *Eur. J. Inorg. Chem.* **2008**, 557–562; i) G. G. Skvortsov, G. K. Fukin, A. A. Trifonov, A. Noor, C. Döring, R. Kempe, *Organometallics* **2007**, 26, 5770–5773; j) A. Noor, R. Kempe, *Eur. J. Inorg. Chem.* **2008**, 2377–2381; k) D. M. Lyubov, C. Döring, G. K. Fukin, A. V. Cherkasov, A. V. Shavyrin, R. Kempe, A. A. Trifonov, *Organometallics* **2008**, 27, 2905–2907; l) A. Noor, F. R. Wagner, R. Kempe, *Angew. Chem.* **2008**, 120, 7356–7359; *Angew. Chem. Int. Ed.* **2008**, 47, 7246–7259; m) A. Noor, W. P. Kretschmer, G. Glatz, A. Meetsma, R. Kempe, *Eur. J. Inorg. Chem.* **2008**, 32, 5088–5098.
- [3] a) K. Müller-Buschbaum, *Z. Anorg. Allg. Chem.* **2003**, 629, 2127–2132; b) C. C. Quitmann, K. Müller-Buschbaum, *Angew. Chem.* **2004**, 116, 6120–6122; *Angew. Chem. Int. Ed.* **2004**, 43, 5994–5996; c) K. Müller-Buschbaum, *Z. Anorg. Allg. Chem.* **2005**, 631, 811–828; d) K. Müller-Buschbaum, C. C. Quitmann, *Inorg. Chem.* **2006**, 45, 2678–2687.
- [4] G. B. Deacon, C. M. Forsyth, P. C. Junk, S. G. Leary, *New J. Chem.* **2006**, 30, 592–596.
- [5] A. M. Dietel, O. Tok, R. Kempe, *Eur. J. Inorg. Chem.* **2007**, 4583–4586.
- [6] We chose this criterion because we expected the metal centers to be close enough to observe NMR coupling.
- [7] P. L. Watson, T. H. Tulip, I. Williams, *Organometallics* **1990**, 9, 1999–2009.
- [8] a) A. G. Avent, P. B. Hitchcock, A. V. Khvostov, M. F. Lappert, A. V. Protchenko, *Dalton Trans.* **2004**, 2272–2280; b) D. M. M. Freckmann, T. Dube, C. D. Berube, S. Gambarotta, G. P. A. Yap, *Organometallics* **2002**, 21, 1240–1246; c) T. Grob, G. Seybert, W. Massa, K. Dehnicke, *Z. Anorg. Allg. Chem.* **2000**, 626, 349–353; d) M. N. Bochkarev, V. V. Khramenkov, Yu. F. Rad'kov, L. N. Zakharov, Yu. T. Struchkov, *J. Organomet. Chem.* **1992**, 429, 27–39; e) G. B. Deacon, C. M. Forsyth, P. C. Junk, B. W. Skelton, A. H. White, *Chem. Eur. J.* **1999**, 5, 1452–1459; f) O. Eisenstein, P. B. Hitchcock, A. V. Khvostov, M. F. Lappert, L. Maron, L. Perrin, A. V. Protchenko, *J. Am. Chem. Soc.* **2003**, 125, 10790–10791; g) J. R. van den Hende, P. B. Hitchcock, M. F. Lappert, *J. Chem. Soc., Dalton Trans.* **1995**, 2251–2258; h) J. R. van den Hende, P. B. Hitchcock, M. F. Lappert, *J. Chem. Soc., Chem. Commun.* **1994**, 1413–1414.
- [9] A. G. Avent, M. A. Edelman, M. F. Lappert, G. A. Lawless, *J. Am. Chem. Soc.* **1989**, 111, 3423–3425.
- [10] See for example: J. F. Berry, F. A. Cotton, C. A. Murillo, *Inorg. Chim. Acta* **2004**, 357, 3847–3853; J. F. Berry, F. A. Cotton, T.

- Lu, C. A. Murillo, *Inorg. Chem.* **2003**, *42*, 4425–4430; L.-G. Zhu, S.-M. Peng, G.-H. Lee, *Chem. Lett.* **2002**, 1210–1211; J. F. Berry, F. A. Cotton, L. M. Daniels, C. A. Murillo, *J. Am. Chem. Soc.* **2002**, *124*, 3212–3213; J. F. Berry, F. A. Cotton, L. M. Daniels, C. A. Murillo, X. Wang, *Inorg. Chem.* **2003**, *42*, 2418–2427; R. Clérac, F. A. Cotton, K. R. Dunbar, C. A. Murillo, I. Pascual, X. Wang, *Inorg. Chem.* **1999**, *38*, 2655–2657; R. Clérac, F. A. Cotton, L. M. Daniels, K. R. Dunbar, K. Kirschbaum, C. A. Murillo, A. A. Pinkerton, A. J. Schultz, X. Wang, *J. Am. Chem. Soc.* **2000**, *122*, 6226–6236.
- [11] M.-M. Rohmer, I. P.-C. Liu, J.-C. Lin, M.-J. Chiu, C.-H. Lee, G.-H. Lee, M. Bernard, X. Lopez, S.-M. Peng, *Angew. Chem. Int. Ed.* **2007**, *46*, 3533–3536.
- [12] T. D. Tilley, R. A. Andersen, A. Zalkin, *Inorg. Chem.* **1984**, *23*, 2271–2276.
- [13] A. Altomare, M. C. Burla, M. Camalli, G. L. Cascarano, C. Giacovazzo, A. Guagliardi, A. G. G. Moliterni, G. Polidori, R. Spagna, *J. Appl. Crystallogr.* **1999**, *32*, 115–119.
- [14] G. M. Sheldrick, *SHELX97*, Program for Crystal Structure Analysis (rel. 97-2), University of Göttingen, Germany, **1998**.
- [15] L. J. Farrugia, *J. Appl. Crystallogr.* **1999**, *32*, 837–838.

Received: October 28, 2008

Published Online: February 3, 2009